

# The impact of synthetic bone grafting for tissue regeneration: an *in vivo* study

Alyaa I. Naser<sup>1\*</sup> , Rayan S. Hamed<sup>1</sup> , Ghada A. Taqa<sup>2</sup> 

<sup>1</sup> Department of Oral and Maxillofacial Surgery, College of Dentistry, The University of Mosul, Iraq.

<sup>2</sup> Department of Dental Basic Sciences, College of Dentistry, University of Mosul, Iraq.

**Corresponding author:**

Alyaa Ismael Naser  
City Mosul, State Nineveh - Iraq  
Postal Code +964  
alyaaismael@uomosul.edu.iq

**Editor:** Dr. Altair A. Del Bel Cury

**Received:** July 7, 2023

**Accepted:** November 30, 2023



**Aims:** This study aimed to examine the biological response of synthetic nanocomposite material on canine mandibular bone.

**Methods:** Nine healthy adult male local breed dogs aged 12 to 18 months and weighing 10.2 to 15.2 kg were used in the study. Based on healing intervals of 1 and 2 months, the dogs were divided into 2 groups. Each group had 3 subgroups with 3 dogs each. The division was based on the grafting material used to fill the created defect: an empty defect (Control-ve), Beta-Tricalcium Phosphate, and nanocomposite (Beta-Tricalcium Phosphate and nanosilver 1%) . Surgery started after the dogs were anaesthetized. The surgical procedure began with a 5 cm parallel incision along the mandible's lower posterior border. After exposing the periosteum, a three 5mm-diameter, 5-mm-deep critical-size holes were made, 5mm between each one. Each group's grafting material had independent 3 holes. The defects were covered with resorbable collagen membranes followed by suturing of the mucoperiosteal flap. **Results:** Total densitometric analysis showed no significant differences between groups at 1-month intervals, with the nanocomposite group having a higher mean rank ( $165.66 \pm 31.21$ ) in comparison to other groups while at 2 months intervals that there was a highly significant difference between three groups as the *P*-value was (0.000) with the nanocomposite group having a higher mean rank ( $460.66 \pm 26.40$ ). **Conclusions:** In the current study, the use of nanocomposites improved osteoconductivity by accelerating new bone formation. Moreover, the incorporation of nanosilver enhanced growth factor activity. These attributes make nanocomposites a promising material for enhancing the bone healing process.

**Keywords:** Calcium phosphates. Cone-beam computed tomography. Anti-bacterial agents. Nanocomposites. Bone substitutes.

## Introduction

After a bone injury, a comprehensive process of bone healing takes place, which is aimed at restoring both the shape and functionality of the bone. This process can be divided into three stages that are closely intertwined and overlap with each other: inflammation, proliferation, and bone remodeling<sup>1,2</sup>. Following an injury, inflammatory cytokines, neutrophils, monocytes, lymphocytes, and macrophages become more polarized. When macrophages become activated, they release inflammatory and chemotactic mediators that attract mesenchymal stem cells (MSCs) from nearby areas to the site of injury. Re-epithelialization, angiogenesis, collagen synthesis, and extracellular matrix (ECM) formation are all processes that occur during the proliferation phase. During the remodeling phase, collagen deposition, vascular maturation, and regression occur<sup>3</sup>. The complications of bone disorders caused by trauma, osteomyelitis, and osteosarcoma continue to be clinically significant<sup>4</sup>. Autologous bone grafts obtained from the rib, iliac crest, or tibia are widely regarded as the most effective method for bone repair. Nevertheless, the use of these grafts necessitates additional surgical procedures, which can lead to various postoperative complications. These complications may include limited availability of donor tissue, donor site morbidity, pain, and the risk of infection<sup>5</sup>. Ideal bone graft materials should have versatile properties like osteoinductive, osteoconductive, and biocompatible, and possess mechanical and structural properties that closely resemble those of natural bone<sup>6</sup>. A common synthetic bioceramic substance used in medical and dental applications is beta-tricalcium phosphate ( $\beta$ -TCP). This biocompatible and resorbable alloplastic bone grafting substance has osteoconductive qualities. This  $\beta$ -TCP has shown complete resorption and replacement by bone within a time frame of roughly 0.5 to 1.5 years when used to treat various bony defects, including intraosseous defects around natural teeth, edentulous defective alveolar ridges, and maxillary sinuses<sup>7,8</sup>. Nanotechnology could revolutionize bone tissue engineering by overcoming bone resorption associated with bone grafting and infection<sup>9</sup>. Moreover, it supplies an osteoconductive, osteoinductive, biocompatible, biodegradable, and bioresorbable bone graft with antibacterial properties<sup>10</sup>. Nanomaterials can be used in maxillofacial surgery as bone replacement materials, prosthetic implants, and dental fillers. A synthetic biomaterial doped with antibacterial metal ions helps to prevent post-operative infections<sup>11</sup>. Silver nanoparticles have been used as nanocomposites in bone cement, scaffolds, and membranes. It has been shown to reduce bacterial colonization and improve dental health. Because of its small size, it may easily pass through bacterial membranes. It is biocompatible and has long-lasting antibacterial activity<sup>12</sup>. The validation of this study was to improve the osteoconductivity of beta-tricalcium phosphate via incorporating nanosilver material within a bone substitute. This study hypothesized that artificial nanocomposite materials would aid bone healing. The objective of this study was to investigate the impact of synthetic nanocomposite material on the biology of canine mandibular bone using CBCT imaging.

## Materials and Methods

### Animals

This study was conducted for two months at the Department of Oral and Maxillofacial Surgery / College of Dentistry / University of Mosul. A total of nine healthy adult

male dogs of the local breed were included in the study. Nine, male local breed, aged 12 to 18 months and weighing between 10.2 and 15.2 kilograms, were obtained from a nearby market. They were housed in cages with adequate ventilation and access to natural light. A veterinarian consultant regularly performed health checks on each dog. The experiment adhered to the guidelines set forth by the National Institutional Health Principles for Laboratory Animal Care (N.I.H. publication no. 85-23, revised 1985). Additionally, the ethical committee thoroughly reviewed and approved the project, considering ethical standards at each stage of the operations and animal handling processes. The approval for the study was granted under the letter of approval No. (UoM.Dent/A.69.22).

## Materials

beta -Tricalcium Phosphate ( $\beta$ -TCP) powder was purchased from Net Granules (Turkey). The silver/beta-tricalcium phosphate nanocomposite bone substitute powder (1%) was bought from Yanhuang Industrial Park (Guanxian, Liaocheng, Shandong, China). The collagen membrane was purchased from Bioplast-Dent Membrane (VALDMIVA/Russia). Straight surgical handpiece that is transportable (Beijing, China).

## Experimental grouping

The study was a **randomized, single-blind experiment** in which the animals were divided into two groups based on the intervals between euthanasia: one month and two months. Each group was divided into three subgroups based on the material implanted into the designated bone defect in the lower border of the jaw (each with three dogs). The following groups are depicted in (Figure 1):

- A. Empty defect (Cont.-ve).
- B.  $\beta$ -tricalcium phosphate.
- C. Nanocomposite.

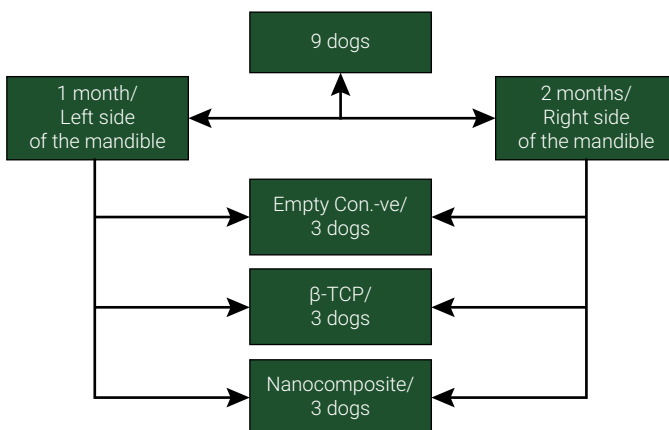


**Figure 1.** Experimental Grouping

## Anaesthesia and Surgical Procedure

To reduce bronchial secretions and support heart rate during anaesthesia, atropine (0.04mg/kg) was administered intramuscularly (Anova/Vietnam). Following that, a mixture of 5% ketamine (Gracure Pharmaceuticals Ltd, Bhiwadi, India) and 2% xylazine (Interchemi Co, Holland) was injected intramuscularly in the thigh muscle using the same syringe. Additional doses of the Ketamine-Xylazine mixture were administered every 30 minutes if necessary to maintain adequate anaesthesia<sup>13</sup>. After the dog had been thoroughly sedated, all hair at the surgical site was removed with a sterilized manual hair removal machine. After that, the surgical area was disinfected by wiping the wound with 10% povidone-iodine. The procedure began with a 5 cm parallel incision on the lower posterior border of the mandible, made with a No. 22 blade on a No. 4 scalpel handle, (Figure 2A). The periosteum was reflected to reveal the mandible's inferior border. Under external normal saline irrigation with a disposable syringe (5 ml), three circular critical-size holes, each 5mm in diameter and depth and 5mm between each one, were created with a 5mm diameter trephine surgical bur and as shown in (Figures 2B, C, D). To standardize the amount of study materials to be placed in each defect, a plastic scoop was used. The first and second groups of defects were filled with study materials (nanocomposite and -tricalcium phosphate, respectively), while the third group defect was left empty being a control (-ve). At completion and to promote uneventful and optimal healing, resorbable collagen membranes were utilized to cover the defects, (Figure 2E). Subsequently, the mucoperiosteal flap and subcutaneous skin were carefully sutured over the affected areas in all dogs using absorbable Vicryl sutures (2/0) to restore it to its original position, (Figure 2F). As a preventive measure against infection and to enhance recovery, the animals received a single intramuscular dose of ceftiofur (5 mg/kg) and diclofenac (3 mg/kg) respectively. Additionally, tetracycline ointment was applied to all skin wounds.

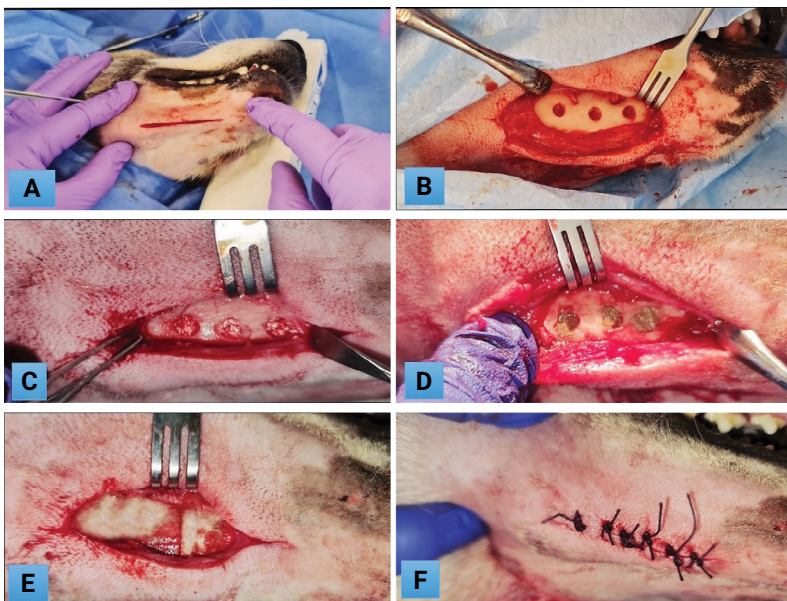


**Figure 2.** Surgical Procedure; A: The incision, B: Con-ve defects, C:  $\beta$ - TCP defects, D : Nanocomposite material defect, E: Collagen membrane, F: Suturing of surgical site.

## Follow-up

For the first twenty-four hours following the procedure, the researchers closely observed and housed the operated animals in separate cages, paying close attention to their diet and activity levels.

## Animals Sacrifice

After two months, nine dogs were euthanized. Pentobarbital was injected intravenously into dogs (1 ml/10 lbs of body weight) to cause their sacrifice. For radiographic analysis, the left mandible was dissected free and fixed in 10% buffered formic acid for two months at a time, and the right mandible for one month at a time.

## Radiographic analysis

Each animal underwent CBCT (Large V/China) scans at both intervals using a CBCT imaging machine. The bone density was estimated in Hounsfield Units (H.U.) utilizing CBCT computer system software. Before exposure, the following parameters were adjusted: kilovoltage (Kv) at 100Kv, milliamp at 6.0 mA, and exposure time at 20 sec. Two radiologists conducted the radiological study by manually selecting the fault location in an axial section using the editing tool, measure, and a three-dimensional (3D) visual inspection. The Mean data from the CBCT scan for each dog was recorded and saved in a digital file format for visualization and analysis purposes.

## Statistical analysis:

The statistical analysis was performed using the Statistical Package for Social Sciences program (SPSS version 22.0, Chicago, IL, U.S.A.). One-way ANOVA was used to compare the three groups within an interval, while independent t-tests were used to compare two independent intervals. The obtained results met a threshold of significance of 5%.

## Results

### Clinical Observations

All skin sutures were removed after 15 days. After surgery, no dogs experienced any complications, either locally or systemically, such as inflammation, foreign-body reactions, or pain.

### Radiographical Results:

A total of 9 dogs had surgery by one surgeon. Six dogs were implanted with different study materials (Nanocomposite,  $\beta$ -tricalcium phosphate) and three dogs were left without treatment (Con -ve group). In total, 27 defects were created in the lower posterior border of the mandible (right side for two months intervals and left side for 1-month intervals). In the present study, the One-way ANOVA test, (Table 1) for 1-month intervals (Figure 3 A) showed no significant difference between groups with a *P*-value (0.291), (Figure 4 1A,1B,1C). In comparison with 2 months intervals, (Figure 3B), one-way ANOVA revealed that there was a highly significant difference

between three groups as the *P*-value was (0.000), (Figure 4 2A, 2B, 2C). The t- independent test (Table 2) between intervals revealed the mean and standard deviation (S.D.) for Con-ve were found to be **(129.33±11.67 and 140±26.21)** in 1 & 2 months, respectively, with *P*- values **(0.55)** with no significant differences between them, (Figure 4 1A,2A). In the β-TCP defects, there was a high significance between the two groups as the mean and standard deviation (S.D.) were found to be **(146±29.00 and 304±41.90)** in 1 & 2 months, respectively, with *P*- values **(0.006)**, (Figure 4 1B, 2B). This was also true for the nanocomposite group, in which there was a high significance between the two groups as the mean and standard deviation (S.D.) being to be **(165.66± 31.21, 460.66±26.40)** in 1 & 2 months, respectively, with *P*-value **(0.000)**, (Figure 4 1C,2C).

**Table 1.** One-way ANOVA for comparison of study groups within the healing period.

Groups	1 month	2 months
Control-ve	129.33±11.67 A	140± 26.21 A
β TCP	146± 29.00 A	304± 41.90 B
Nano	165.66± 31.21 A	460.66± 26.40 C
P-Value	<b>0.291</b>	<b>0.000*</b>

Different letters among material groups through the same healing period in columns mean there is a significant difference at *P*≤0.05.

**Table 2.** Independent t-test for comparison of study groups during healing periods.

Times	Control	βTCP	Nano
1 <sup>st</sup> month	129.33±11.67	146±29.00	165.66± 31.21
2 <sup>nd</sup> month	140±26.21	304±41.90	460.66±26.40
P-Value	<b>0.55</b>	<b>0.006*</b>	<b>0.000*</b>

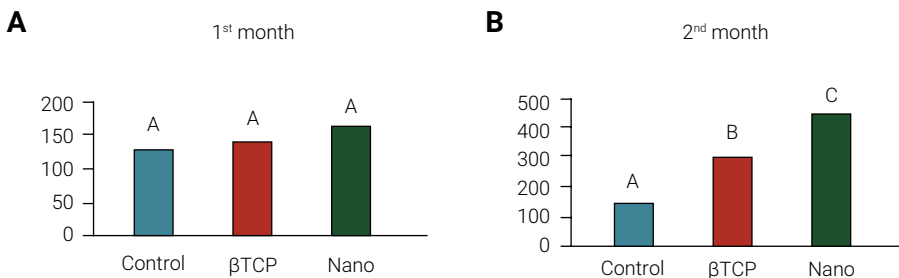


**Figure 3.** One-way ANOVA for comparison of study material within groups, A: (one month) and B: (two- months)



**Figure 4.** Cone beam compared tomography in the axial plane of the surgical defects representing the study groups at two healing periods. A:Con-ve, B:  $\beta$ - TCP, C:Nanocomposite.

## Discussion

This study aimed to compare the enhancement of bone densities using synthetic nanocomposite bone substitutes versus  $\beta$ -TCP and as assessed by CBCT. Several animal models have been proposed for bone graft research. In the present study, adult local breed dogs were utilized as experimental subjects. Choosing large animals like dogs over rabbits or rats offers several advantages, primarily due to their ability to provide bone defects of sufficient size to accommodate a diverse range of graft materials for evaluating different assessment methods<sup>14</sup>. Large animal models offer authentic disease models that closely resemble the conditions observed in humans, including genetic and physiological variations and complex interactions with the environment. This similarity allows for more accurate assessments of the safety and effectiveness of new treatments<sup>15</sup>.

In this current investigation, bone density was evaluated using CBCT. The findings align with a previous study conducted by Razi et al.<sup>16</sup>, suggesting that grey values can be effectively utilized for measuring bone density. Razi and his colleagues concluded from their study comparing the Hounsfield Unit (HU) in computed tomography (CT)

with the grey level in CBCT in human tissues that there was a high degree of agreement between HU in CT and grey level in CBCT in both hard and soft tissues and that it can be used as a parameter to determine bone density in implant treatment as well as to determine bone type, due to its low radiation dose, short time, and low cost compared to CT<sup>17</sup>.

To the best of our knowledge, this study represents one of the attempts to compare the effectiveness of nanocomposite synthetic bone substitutes versus  $\beta$ -TCP in enhancing bone density using CBCT. In the current study, the results of CBCT radiography for the study groups at one-month intervals showed the presence of a radiolucent zone of defects equal to some extent in the (Con-ve,  $\beta$ -TCP nanocomposite) groups, with a higher mean in the nanocomposite group ( $165.66 \pm 31.21$ ). This radiolucency decreased overtime with a shift to a higher rate of new bone formation. The body's defence against materials induces inflammatory reactions as a normal healing process. However, this reaction subsided in the nanocomposite group and as it has an antibacterial effect due to the presence of nanosilver. The effect of silver nanoparticles (AgNPs), a part of nanocomposite material composition that reduces post-operative bacterial contamination, promotes a higher bone deposition rate, and increases the defects' radiopacities. Based on these assumptions, many studies assessed the bactericidal effect of silver nanoparticles. They concluded that the strong positive effect of Ag NPs incorporating biomaterials like beta-tricalcium phosphate reduces post-operative bacterial contamination<sup>18</sup>.

AgNPs can traverse the outer membrane, gather within the inner membrane, and engage with sulfur or phosphorus groups, leading to cell destabilization and harm. This process heightens the permeability of the membrane, ultimately causing cell demise<sup>19</sup>. The findings of this study were consistent with the findings of Bee et al.<sup>20</sup>, who concluded that the addition of silver nanoparticles to hydroxyapatite exhibits optimal antibacterial and bioactive properties and has the potential to be used as an implant material for dental and orthopaedic applications.

At second-month- intervals, the nanocomposite group showed a superior biological response in comparison with  $\beta$ - TCP and the control group with a *P*-value (0.000) and higher mean value ( $460.66 \pm 26.40$ ). The defects appeared more radiopac and decreased in size. This could be due to the prolonged release of nano beta-tricalcium phosphate which accelerates bone formation owing to its impact on osteoblastic behaviour and the presence of nanosilver which helps when combined with a variety of biomaterials to significantly release growth factors<sup>21,22</sup>. Furthermore, AgNPs exhibit remarkable effects on guided bone regeneration by facilitating the initial stage of bone repair through their involvement in the gene expression of fibroblast growth factor (FGF).

This stimulation causes blood vessel and fibroblast proliferation and differentiation, as well as the activation of vascular endothelial growth factor (VEGF), which aids in the proliferation and organization of endothelial cells involved in angiogenesis<sup>23</sup>. In addition, nano beta-tricalcium phosphate promotes the formation of blood vessels shortly after implantation, which in turn facilitates the induction of osteoblasts and osteoclasts within the macropores. Moreover, these particles attract osteoprogenitor cells, which migrate into the interconnecting micropores of the bone substitute mate-

rial. Once there, these cells differentiate into osteoblasts, leading to the deposition of new bone.<sup>24</sup> These results are in line with those of Zhang et al.<sup>25</sup>, who found that when beta-tricalcium phosphate biomaterials are stimulated, macrophages express fewer inflammatory factors (IL-1), produce more anti-inflammatory cytokines (IL-10, IL-1 $\alpha$ ), and produce growth factors (VEGF, PDGF, EGF, BMP-2, and TGF- $\beta$ 1) that collectively result in a pro-osteogenic microenvironment.

The clinical relevance of this study is to improve the osteoconductive property of artificial bone substitutes through the sustained release of beta-tricalcium phosphate and nanosilver. In implant dentistry, these properties will aid in increasing the success rate of implant by improving its primary stability when using bone graft with it.

The limitations of this study were that the healing periods was relatively short suggesting a longer period. In addition, CBCT image acquisition was difficult to control as the bone specimens were uncoordinate in shape.

In conclusion, the properties and modifications of nanocomposites are closely associated with their effectiveness in exhibiting biocompatibility, osteoconductivity and antibacterial activity. These attributes make nanocomposites promising for enhancing bone healing processes.

## Acknowledgement

Exceptional appreciation to the College of Dentistry, University of Mosul, and Department of Oral and Maxillofacial Surgery for their support to conduct this study.

## Declaration of Interest

The authors declare that they have no conflict of interest.

## Source of funding

This research did not receive any specific funding.

## Author Contribution

**Alyaa I. Naser:** Concepts, data curation, analysis, research, methodology, resources, software, supervision, validation, display, writing – original draft, drafting – revision and editing.

**Rayan S. Hamed:** Concepts, data curation, analysis, research, methodology, resources, software, supervision, validation, display, writing – original draft, drafting – revision and editing.

**Ghada A. Taqa:** Concepts, data curation, analysis, research, methodology, resources, software, supervision, validation, display, writing – original draft, drafting – revision and editing.

All authors actively participated in the manuscript's findings, revised, and approved the final version of the manuscript.

The authors disclose whether they used artificial intelligence (AI)-assisted technologies (such as Large Language Models [LLMs], chatbots, or image creators) in the production of submitted work.

---

## References

1. Zamfirescu AI, Banciu A, Banciu D, Jinga SI, Busuioc C. Composite fibrous scaffolds designed for bone regeneration. *Rom J Mater*. 2020 Apr;50(2):161-5.
2. Schell H, Duda GN, Peters A, Tsetsilonis S, Johnson KA, Schmidt-Bleek K. The haematoma and its role in bone healing. *J Exp Orthop*. 2017 Dec;4(1):5. doi: 10.1186/s40634-017-0079-3.
3. Medhat D, Rodríguez CI, Infante A. Immunomodulatory Effects of MSCs in Bone Healing. *Int J Mol Sci*. 2019 Nov;20(21):5467. doi: 10.3390/ijms20215467.
4. Borrelli MR, Hu MS, Longaker MT, Lorenz HP. Tissue Engineering and Regenerative Medicine in Craniofacial Reconstruction and Facial Aesthetics. *J Craniofac Surg*. 2020 Jan/Feb;31(1):15-27. doi: 10.1097/SCS.0000000000005840.
5. Kattimani V, Lingamaneni KP, Chakravarthi PS, Kumar TS, Siddharthan A. Eggshell-Derived Hydroxyapatite: A New Era in Bone Regeneration. *J Craniofac Surg*. 2016 Jan;27(1):112-7. doi: 10.1097/SCS.0000000000002288.
6. Tebyanian H, Norahan MH, Eyni H, Movahedin M, Mortazavi SJ, Karami A, et al. Effects of collagen/ $\beta$ -tricalcium phosphate bone graft to regenerate bone in critically sized rabbit calvarial defects. *J Appl Biomater Funct Mater*. 2019 Jan-Mar;17(1):2280800018820490. doi: 10.1177/2280800018820490.
7. Jasser RA, AlSubaie A, AlShehri F. Effectiveness of beta-tricalcium phosphate in comparison with other materials in treating periodontal infra-bony defects around natural teeth: a systematic review and meta-analysis. *BMC Oral Health*. 2021 Apr 29;21(1):219. doi: 10.1186/s12903-021-01570-8.
8. Hayashi K, Kishida R, Tsuchiya A, Ishikawa K. Granular honeycombs composed of carbonate apatite, hydroxyapatite, and  $\beta$ -tricalcium phosphate as bone graft substitutes: effects of composition on bone formation and maturation. *ACS Appl Bio Mater*. 2020 Mar;3(3):1787-95. doi: 10.1021/acsabm.0c00060.
9. Umopathy VR, Natarajan PM, Sumathi Jones C, Swamikannu B, Johnson WM, Alagarsamy V, et al. Current trends and future perspectives on dental nanomaterials - An overview of nanotechnology strategies in dentistry. *J King Saud Univ Sci*. 2022 Oct;34(7):102231. doi: 10.1016/j.jksus.2022.102231.
10. Kupikowska-Stobba B, Kasprzak M. Fabrication of nanoparticles for bone regeneration: new insight into applications of nanoemulsion technology. *J Mater Chem B*. 2021 Jul;9(26):5221-44. doi: 10.1039/d1tb00559f.
11. Fuh LJ, Huang YJ, Chen WC, Lin DJ. Preparation of micro-porous bioceramic containing silicon-substituted hydroxyapatite and beta-tricalcium phosphate. *Mater Sci Eng C Mater Biol Appl*. 2017 Jun;75:798-806. doi: 10.1016/j.msec.2017.02.065.
12. Chen J, Ashames A, Buabeid MA, Faelelbom KM, Ijaz M, Murtaza G. Nanocomposites drug delivery systems for the healing of bone fractures. *Int J Pharm*. 2020 Jul;585:119477. doi: 10.1016/j.ijpharm.2020.119477.
13. Allawi AH, Alkattan LM, Aliraqi OM. Clinical and ultrasonographic study of using autogenous venous graft and platelet-rich plasma for repairing Achilles tendon rupture in dogs. *Iraq J Vet Sci*. 2019;33(2):453-60. doi: 10.33899/IJVS.2019.163199.

14. Mourão CF, Lowenstein A, Mello-Machado RC, Ghanaati S, Pinto N, Kawase T, et al. Standardization of animal models and techniques for platelet-rich fibrin production: a narrative review and guideline. *Bioengineering (Basel)*. 2023 Apr;10(4):482. doi: 10.3390/bioengineering10040482.
15. Ribitsch I, Baptista PM, Lange-Consiglio A, Melotti L, Patruno M, Jenner F, et al. Large Animal Models in Regenerative Medicine and Tissue Engineering: To Do or Not to Do. *Front Bioeng Biotechnol*. 2020 Aug;8:972. doi: 10.3389/fbioe.2020.00972.
16. Razi T, Emamverdizadeh P, Nilavar N, Razi S. Comparison of the Hounsfield unit in CT scan with the gray level in cone-beam CT. *J Dent Res Dent Clin Dent Prospects*. 2019 Summer;13(3):177-82. doi: 10.15171/joddd.2019.028.
17. Kamaruddin N, Rajion ZA, Yusof A, Aiz ME. Relationship between Hounsfield unit in CT scan and gray scale in CBCT. *AIP Conf Proc*. 2016;1791:020005. doi: 10.1063/1.4968860.
18. Pokrowiecki R, Wojnarowicz J, Zareba T, Koltsov I, Lojkowski W, Tyski S, et al. Nanoparticles and human saliva: a step towards drug delivery systems for dental and craniofacial biomaterials. *Int J Nanomedicine*. 2019 Nov;14:9235-57. doi: 10.2147/IJN.S221608.
19. Menichetti A, Mavridi-Printezi A, Mordini D, Montalti M. Effect of size, shape and surface functionalization on the antibacterial activity of silver nanoparticles. *J Funct Biomater*. 2023 Apr;14(5):244. doi: 10.3390/jfb14050244.
20. Bee SL, Bustami Y, Ul-Hamid A, Lim K, Abdul Hamid ZA. Synthesis of silver nanoparticle-decorated hydroxyapatite nanocomposite with combined bioactivity and antibacterial properties. *J Mater Sci Mater Med*. 2021 Aug;32(9):106. doi: 10.1007/s10856-021-06590-y.
21. Slane J, Vivanco J, Rose W, Ploeg HL, Squire M. Mechanical, material, and antimicrobial properties of acrylic bone cement impregnated with silver nanoparticles. *Mater Sci Eng C Mater Biol Appl*. 2015 Mar;48:188-96. doi: 10.1016/j.msec.2014.11.068.
22. Bruna T, Maldonado-Bravo F, Jara P, Caro N. Silver Nanoparticles and Their Antibacterial Applications. *Int J Mol Sci*. 2021 Jul 4;22(13):7202. doi: 10.3390/ijms22137202.
23. Crisan CM, Mocan T, Manolea M, Lasca LI, Tăbăran FA, Mocan L. Review on silver nanoparticles as a novel class of antibacterial solutions. *Applied Sciences*. 2021 Jan;11(3):1120. doi:10.3390/app11031120.
24. Ahmed WS, Sherif HA, Nasr GA. Evaluation of the effect of beta-tri-calcium phosphate nano particles on bone defect healing in diabetic rats (Histological study). *Al-Azhar J Dent Sci*. 2019 Jan;22(1):87-93. doi:10.21608/ajdsm.2019.71725.
25. Zhang Y, Shu T, Wang S, Liu Z, Cheng Y, Li A, et al. The osteoinductivity of calcium phosphate-based biomaterials: a tight interaction with bone healing. *Front Bioeng Biotechnol*. 2022 May;10:911180. doi: 10.3389/fbioe.2022.911180.